

Original Research Article

COMPUTATIONAL CHEMISTRY STUDIES ON THE ADSORPTION/CORROSION INHIBITIVE POTENTIAL OF 2-(2-heptadecyl-4,5-dihydro-1H-imidazol-1-yl) ethan-1-ol ON IRON SURFACE AT DIFFERENT TEMPERATURES

ABSTRACT

A computational study on 2-(2-heptadecyl-4,5-dihydro-1H-imidazol-1-yl) ethan-1-ol (HDDH) was carried out to determine the adsorption/corrosion inhibitive potential at the temperatures of 60 °C and 80 °C on iron surface using the Material Studio software. For this purpose, Molecular dynamic simulation and quantum chemical calculation was used to calculate different chemical parameters such as the energy of the highest occupied molecular orbital (E_{HOMO}), energy of the lowest unoccupied molecular orbital (E_{LUMO}), ionization potential (IE), electronegativity (χ), electron affinity (EA), global hardness (η), global softness (σ), number of electron transfer (ΔN), electrophilicity index (ω), dipole moment (μ), energy of deformation (Δ), van der Waal accessible surface (λ), others include interaction energy, binding energy, molecular energy and distance between HDDH and iron surface, to predict the adsorption/corrosion inhibitive potential of HDDH. The results show that HDDH uses the ring part of the molecule to adsorb on the iron surface with the N=C-N region in the ring as its most active site. Both the Molecular Dynamic Simulation and Quantum Chemistry Calculation methods confirms HDDH to adsorb/inhibit better at 60 °C with a higher binding energy of 190 Kcal/mol and a smaller energy gap of 4.086 eV just to mention a few. The molecule is physically adsorbed on the iron surface.

Keywords: *Molecular Dynamic Simulation, Quantum Chemical Calculations, Iron, adsorption, 2-(2-heptadecyl-4,5-dihydro-1H-imidazol-1-yl) ethan-1-ol(HDDH). Corrosion Inhibitive*

1. INTRODUCTION

The period in human history beginning in about 1200 B.C. is called the Iron Age. It was about this time that humans started using iron metal. On the other hand, one could refer to this present era as the New Iron Age. Iron in all probability is the most important and the

most widely used metal today. No other metal is available to replace iron in all its many applications. This has resulted in the research into its corrosion resistance in various aggressive environment. Amine and its derivatives are well known as corrosion inhibitors for iron and its alloys, their relatively high water solubility is an advantage for their use as inhibitors [1]. It has been discovered that most organic inhibitors act by adsorption of the metal surface [2]. Imidazoline and its derivatives are typical amine-nitrogen compound which are heterocyclic in nature and possess some heteroatoms which aids adsorption on a metal surface thereby reducing its dissolution, [3] because the lone electron pairs of electron in the hetero atoms and the planarity of a molecule are important features that determine the adsorption of molecules on a metallic surface [4] and are assumed to be the active sites. Nevertheless, in the case of physisorption increase in temperature reduces inhibitor efficiency due to its desorption from the metal surface [5]. Thus, finding an inhibitor with high efficiency at low and high temperatures is of substantial economic significance.

Computational chemistry uses mathematical approximation and computer programs to obtain results relative to chemical problems. It uses methods of theoretical chemistry, incorporated into efficient computer programs, to calculate the structures and properties of molecules and solids. These theoretical methods include Molecular dynamic simulation which is very important for understanding structural changes, interactions and energetics of molecules, and Quantum chemical calculation which uses quantum mechanics to solve the structures, energetic and the reactivity's of molecules. Theoretical methods have been used to determine the adsorption/corrosion inhibitive properties of different molecules such as the work reported on Triazoles and Benzimidazole derivatives [6], Vinyl Imidazole derivatives [7], Quinoxaline derivatives [8], and some Shift bases [9] just to mention a few.

In this study, the adsorption/corrosion inhibitive potential of the imidazoline derivative 2-(2-heptadecyl-4,5-dihydro-1H-imidazol-1-yl) ethan-1-ol (HDDH) will be studied at the structure at geometry optimization and the best equilibrium structures obtained at the temperatures of 60 °C and 80 °C in a vacuum/gas phase acidic environment with more emphasis lay on the equilibrium structures at 60 °C and at 80 °C to determine at what temperature it adsorb/inhibit better. A deeper understanding of the contribution of each of the main atoms and bonds present in HDDH will be known. The chemical structure of the compound studied is shown in Fig. 1.

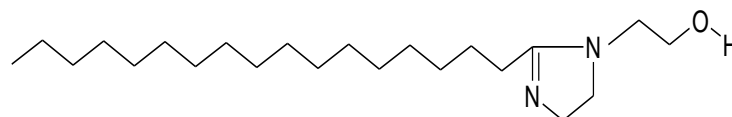


Fig. 1. Schematic structure of 2-(2-heptadecyl-4,5-dihydro-1H-imidazol-1-yl) ethan-1-ol (HDDH)

2. COMPUTATIONAL DETAILS

The Forcite, Vamp and the Dmol³ module present in the Material Studio software which was developed by Accelrys Incorporation San Diego California was used. This software is a high quantum mechanical computer program. The Molecular Dynamic Simulation was done using the Forcite module (which is an advanced classical molecular mechanical tool that allows fast energy calculations and reliable geometry optimization of molecules and periodic system) in a simulation box with dimension (length of 20.1 Å x breadth of 8.6 Å and height of 34.4 Å) with a periodic boundary conditions to model a representative part of the interface devoid of any arbitrary effects. The box consists of an iron slab and a vacuum layer of height 28.1 Å. The Fe crystal was cleaved along the (001) plane with the topmost layer released and the internal layer fixed. The Molecular dynamic simulation was done at the temperatures of 60 °C and 80 °C respectively. The number of particles and the volume of each system in

the ensemble are constant and the ensemble has a well-defined temperature (NVT Ensemble) with a time step of 0.1 fs and simulation time of 5ps to show the effect of change in temperatures on the molecule properties. The values of the interaction energy of the molecule with the Fe (001) surface was calculated using the equation provided by Xia [10]

$$E_{\text{Fe-molecule}} = E_{\text{complex}} - E_{\text{Fe}} - E_{\text{molecule}} \quad (1)$$

E in equation (1) stands for energy so therefore $E_{\text{Fe-molecule}}$ is the interaction energy, E_{complex} is the total energy of the Fe crystal together with the adsorbed molecule, E_{Fe} is the total energy of the Fe crystal and E_{molecule} is the total energy of the adsorbed molecule. The binding energy is said to be the negative energy of the interaction energy as shown in equation 2

$$E_{\text{binding}} = - E_{\text{Fe-molecule}} \quad (2)$$

The force field CVFF (Consistent Valence Force Field) was used for the simulation operation. It is mainly used for the study of structures and binding energy, though it can also accurately predict vibrational frequencies and conformation energy.

The Quantum chemical calculations were done using the Vamp module which is a semi empirical molecular orbital package for organic and inorganic system, [11] and the Dmol³ module which is program which uses the density functional theory (DFT) with a numerical radial function basis set to calculate the electronic properties of molecule cluster surface and crystalline solid material from the first principle [12]. Using the Vamp module theoretical calculations were carried out at the restricted Hartree-fock level (RHF) using the parametric method 3 (PM3) which is based on the neglect of diatomic differential overlap (NDDO) approximation. Using the Dmol³ module calculations were performed using the DFT method in combination with the BLYP (from the name Becke for the exchange part and Lee, Yang and Parr for the correlation part) functional method via the DNP (Double numeric with polarization) basic set which is the best basic set in Dmol³ module [13]. The molecular properties that were well reproduced by DFT/BLYP includes the energy of the highest occupied molecular orbital (E_{HOMO}), energy of the lowest unoccupied molecular orbital (E_{LUMO}), ionization potential (IE), electronegativity (χ), electron affinity (EA), global hardness (η) and global softness (σ) etc. These quantities are often defined using Koopmans's theorem [14] the ionization potential (IE) and the electron affinity (EA) of the molecule are given as

$$IE = - E_{\text{HOMO}} \quad (3)$$

$$EA = - E_{\text{LUMO}} \quad (4)$$

Hence, the values of the electronegativity (χ) and the global hardness (η) according to Pearson operational and approximation definitions can be calculated using the following relations [15]

$$\chi = \frac{IE + EA}{2} \quad (5)$$

$$\eta = \frac{IE - EA}{2} \quad (6)$$

Electron polarizability, also called global softness (σ) is the measure of the capacity of an atom or group of atoms to receive electrons [15] it is evaluated as the reciprocal of the global hardness as shown in equation (7)

$$\sigma = \frac{1}{\eta} \quad (7)$$

When two systems, Fe and a molecule are brought together, electrons will flow from lower electronegative (χ) molecule to higher electronegative (χ) Fe, until the chemical potentials become equal. Therefore, the fraction of electrons transferred (ΔN) from the molecule to the metallic atom was calculated according to Pearson electronegativity scale [16]

$$\Delta N = \frac{\chi_{\text{Fe}} - \chi_{\text{mole}}}{2(\eta_{\text{Fe}} + \eta_{\text{mole}})} \quad (8)$$

Where χ_{Fe} and χ_{mole} is the electronegativity of iron and the molecule respectively, while η_{Fe} and η_{mole} is the global hardness of iron and the molecule respectively. The theoretical values of $\chi_{\text{Fe}} = 7.0$ eV and $\eta_{\text{Fe}} = 0$ was used for this calculation. Parr *et al.* [17] also introduced an electrophilicity index (ω) which is given as

$$\omega = \frac{\chi^2}{2\eta} \quad (9)$$

This is the electrophilic power of a molecule. i.e. the higher the value of ω , the higher the ability of the molecule to accept electrons. This reactive index measures the stabilization in energy when a system gain an additional electronic charge ΔN from the environment.

The local reactivity of the molecule was studied using the Fukui indices [18]. The Fukui indices are measures of chemical reactivity, as well as an indicative of the reactive regions for electrophilic and nucleophilic attack on the molecule. The region of a molecule where the Fukui function is large is chemically softer than the region where the Fukui function is less. The change in electron density is the electrophilic $f^-(r)$ and nucleophilic $f^+(r)$ Fukui functions, which can be calculated using the finite difference approximation as follows [19]

$$f_k^+ = q_{N+1} - q_N \quad (10)$$

$$f_k^- = q_N - q_{N-1} \quad (11)$$

where q_N , q_{N+1} and q_{N-1} are the electronic population of the atom k in neutral, anionic and cationic system. The N stands for the number of electrons in the molecule, $N+1$ stands for an anion with an electron added to the LUMO of the neutral molecule, while $N-1$ stands for the cation with an electron remove from the HOMO of the neutral molecule.

In this study, the molecule was sketched the hydrogens were adjusted and the molecule was cleaned, these were done using the sketch tool available in the material visualizer. All calculations were done on the molecular structure obtained at geometry optimization, 60 °C and 80 °C. The colour codes for the atoms in the molecule are gray for carbon, white for hydrogen, red for oxygen and blue for nitrogen.

3. RESULTS AND DISCUSSION

3.1 Molecular Dynamic Simulation

The close contacts as well as the best adsorption configuration consisting of the molecule HDDH interacting with the iron surface is shown in Fig. 2. Resulting in the modes of adsorption of HDDH with the iron surface at geometry optimization, 60 °C and 80 °C. Equilibration of the system at 60 °C and 80 °C is brought about by the steady average values of energy as well as temperature [10]. From Fig. 2. it is seen that the ring part of HDDH is shown to lay plainly on the iron surface while the alkyl hydrophobic tail deviates from the metal surface thereby creating a barrier between the iron surface and the agents of corrosion

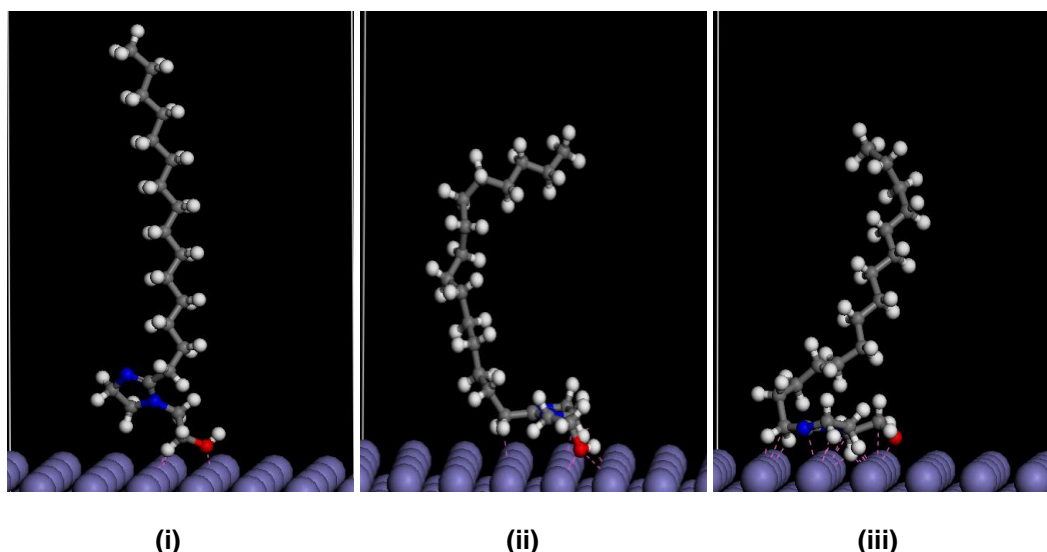


Fig. 2. Modes of adsorption of HDDH at (i) Geometry optimization (ii) 60 °C and (iii) 80 °C

The values of the interaction energies are shown in Table 1. The more negative the interaction energy the higher the binding energy, so also the stronger the bonding between HDDH and the iron surface, the easier HDDH is adsorbed on the iron surface resulting in a better adsorption/corrosion inhibitive effect. HDDH show a more negative interaction hence a higher binding energy at 60 °C. The geometry optimized structure and the equilibrium structures of HDDH at 60 °C and 80 °C are shown in Fig. 3. The system is said to be at the lowest energy state at geometry optimization. The entropy of the molecule at this state can be said to be equal to zero. The entropy of the structure at equilibrium (structure of the molecule at 60 °C and 80 °C) increases due to temperature. It's the same molecule that is brought about by the equilibration of the system in Fig. 2. Table 1. shows the energy of the molecule at geometry optimization to be lower than the energy at the equilibrium structure, this is because the temperature at equilibrium increases the entropy of the atoms in the molecule which leads to an increase in the energy of the system (molecule). The geometry optimized structure is the most stable structure considering the molecular energy calculations followed by the equilibrium structure at 60 °C. Table 1. also shows the minimum distance between HDDH and the iron surface in Armstrong unit (Å). From Table 1. it is seen that the minimum distance between HDDH and the iron surface is greater than 3 Å ($d > 3 \text{ Å}$) which suggest that HDDH is physically adsorbed on the iron surface [20, 21]. The distance at 80 °C is higher than at 60 °C, this may be because of the increase in temperature which aids desorption of HDDH on the iron surface.

Table 1. Interaction energy, binding energy, molecular energy and distance between HDDH and iron surface at 60 °C and 80 °C.

Energies and Distance Parameters	Geo Opt	60 °C	80 °C
Interaction Energy (Kcal/mol)		-190	-186
Binding Energy (Kcal/mol)		190	186
Molecular Energy (Kcal/mol)	54	133	140
Distance between HDDH and Fe (Å)		3.056	3.222

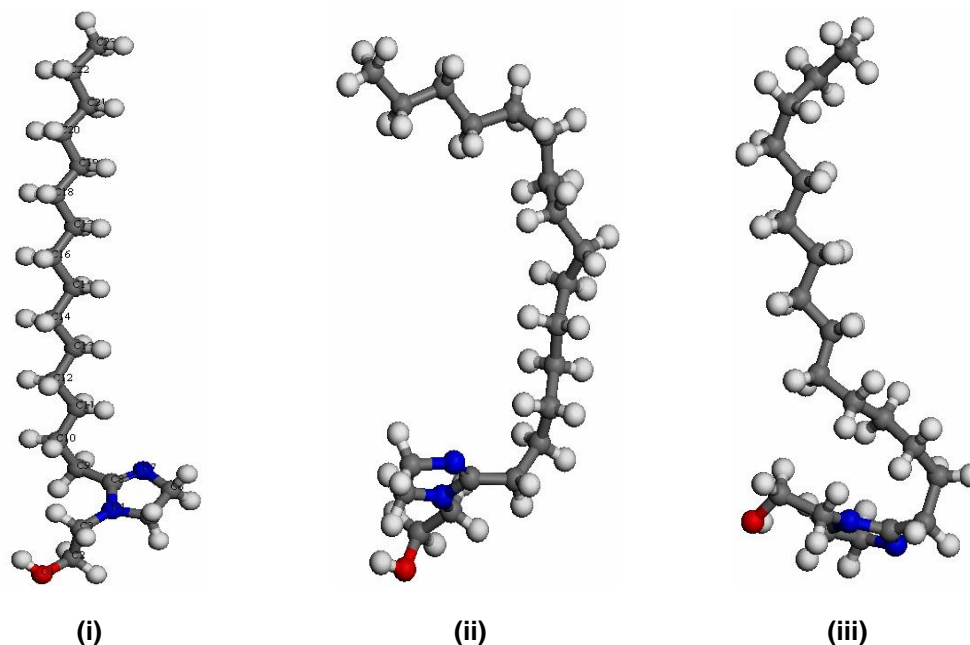


Fig. 3. Structures of HDDH at (i) Geometry optimization, Equilibrium structures at (ii) 60 °C and at (iii) 80 °C.

3.1.1. Bond Length Analysis and Natural Atomic Charge

Fig. 4. shows the bond length in Armstrong unit (Å) for the geometry optimized and the equilibrium structures of HDDH. It is observed that the structural changes seen by HDDH at geometry optimization and at the equilibrium structures is due to the change in bond length observed between the atoms present in HDDH. It is observed that the N=C8 atoms has a shorter bond length compared to the others. Atoms bonded to the heteroatoms shows shorter bond length compared to the C-C bond. This means that the closer the nuclei of the bonding atoms the greater the supply of energy to break the bond between them due to the large force of attraction between the atoms, hence the higher the chemical reactivity of the bond. Therefore, shorter bond length has a higher bond energy and reactivity

Chemical interaction could be by electrostatic or orbital interaction. Fig. 5. shows the natural atomic charges in Coulombs (C) for HDDH, it is observed that the C8 atom is positively charged. This may be due to the inductive effect between the C8 atom which is between the N4 and N7 atom making the C-N bond strongly polarized towards the Nitrogen atom. The Oxygen and Nitrogen heteroatoms involves are more negative than the carbon atoms. The high charge in C23 may be due to dipole moment (uneven distribution of charges) observed between the last carbon atom and the last hydrogen atom. The charges at the equilibrium structure is observed to be higher for most of the atoms compared to the charges at geometry optimization. The hydrogen atoms present in HDDH are all positively charged.

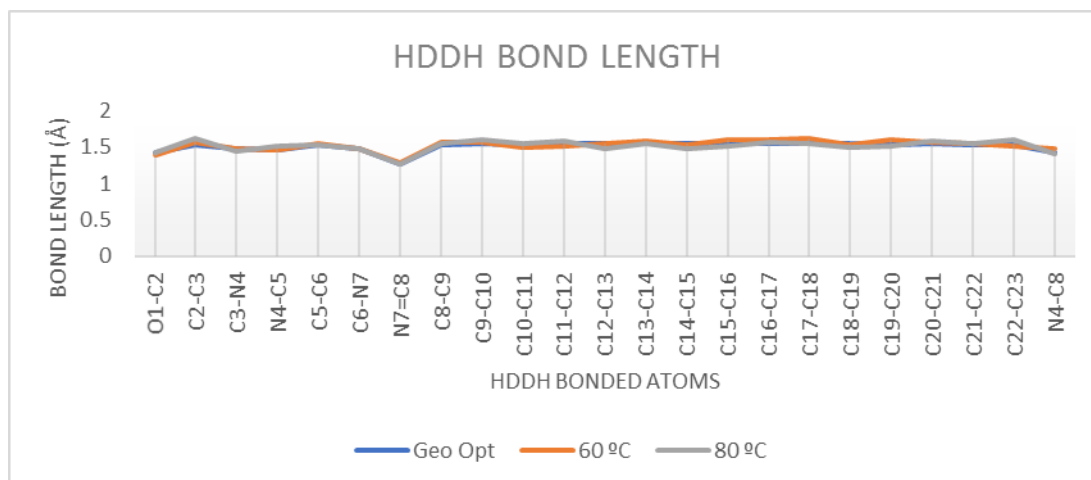


Fig. 4. Bond length analysis for HDDH at Geometry Optimization, 60 °C and 80 °C

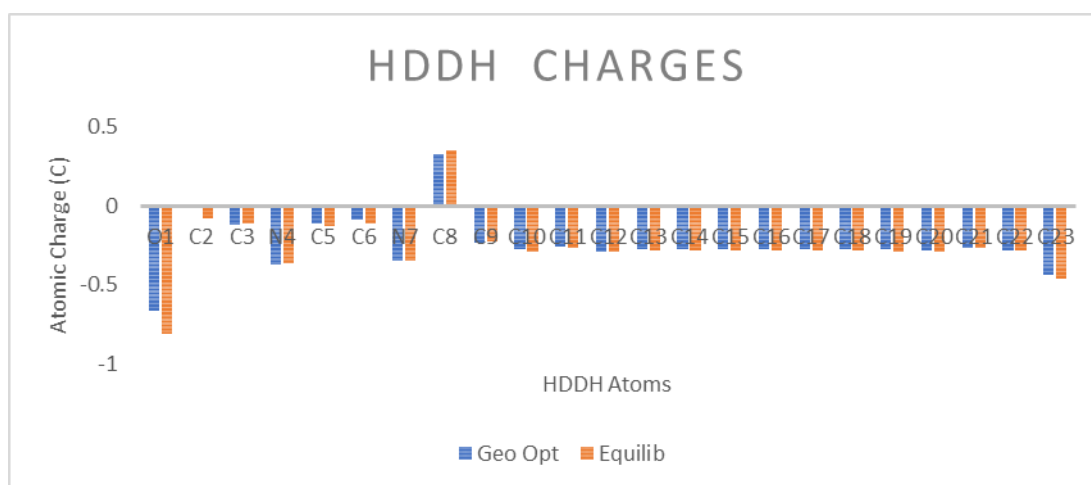


Fig. 5. Natural atomic charge for HDDH at geometry optimization and at equilibrium

3.2 Quantum Chemical Calculation

To have a deeper understanding of the adsorption/corrosion inhibitive potential of HDDH with iron surface the quantum chemical calculations was performed. The calculated Quantum chemical parameters such as dipole moment (μ), energy of deformation (D), van der Waal accessible surface (λ), energy of the highest occupied molecular orbital (E_{HOMO}), energy of the lowest unoccupied molecular orbital (E_{LUMO}), energy gap (ΔE), ionization potential (IE), electronegativity (χ), electron affinity (EA), global hardness (η) and global softness (σ), number of electron transfer (ΔN) and electrophilicity index (ω) can be seen in Table 2. According to the frontier molecular orbital theory (FMO), transition of electron is brought about by the interaction between the highest occupied molecular orbital and the lowest unoccupied molecular orbital. The HOMO is the electron donating ability of a molecule, while the LUMO indicates the ability to accept electron. Therefore, higher values of E_{HOMO} indicates better tendency towards the donation of electron, thereby enhancing the adsorption of the molecule on iron surface and therefore better inhibition efficiency. From Table 2. HDDH has the highest HOMO energy at 60 °C indicating better adsorption/corrosion inhibitive efficiency at that temperature. The negative

signs observed on the values of E_{HOMO} shows that the adsorption is physisorption [22]. This is in line with the assumption made concerning the distance observed between HDDH and the Fe surface (Table 1.) that the adsorption observed by the molecule on the Fe surface may be physisorption. The molecule is also said to accept electrons from the empty d-orbital of iron. The energy difference between the HOMO and the LUMO orbital called the energy gap (ΔE) which is calculated as ($\Delta E = E_{LUMO} - E_{HOMO}$) and it is a very important parameter in that it provides information about the overall reactivity of a molecule; the smaller the ΔE value is, the greater is the reactivity of a molecule [23]. The results presented in Table 2. shows HDDH to have the smallest energy gap at 60 °C indicating a higher reactivity of HDDH at that temperature with the iron surface. The HOMO and LUMO orbital plots for the most stable state of the molecule (geometry optimization) is shown in Fig. 5. it can be observed that the HOMO density plot is more on the ring part of the molecule than at the pendent part. The tail part of HDDH shows no HOMO or LUMO orbital plots which indicates that this part of the molecule will not be responsible for adsorption. We can say that the part of the molecules with high HOMO density will be oriented toward the iron surface as seen in Fig. 2. The LUMO is shown to be also in the ring but also in the atoms connecting the ring and the tail part of the molecule. Note that the blue and yellow isosurface depict the electron density difference; the blue regions show electron accumulation, while the yellow regions show electron loss.

Table. 2. Quantum Chemical Parameters for HDDH at Geometry Optimization, 60 °C and 80 °C

Quantum parameter	Geo Opt	60 °C	80 °C
$E_{HOMO}(eV)$	-4.329	-4.076	-4.338
$E_{LUMO}(eV)$	0.148	0.010	-0.022
$\Delta E \text{ gap}(eV)$	4.477	4.086	4.316
μ (Debye)	2.798	3.664	4.234
D (eV)	1533.8	1556.0	2171.1
EA (eV)	-0.148	-0.010	0.022
IE (eV)	4.329	4.076	4.338
λ (\AA^2)	483.573	484.820	473.608
χ (eV)	2.091	2.033	2.180
η	2.24	2.04	2.16
σ	0.45	0.49	0.46
ΔN	1.10	1.22	1.12
ω	0.98	1.01	1.10

The dipole moment is an important electronic parameter in terms of the reactivity of a molecule, but is not a significant parameter in this context, due to the fact that some work does report that higher dipole moment means higher reactivity [24] while other has reported that lower dipole moment means higher reactivity [25]. The deformation energy on the other hand is the energy required to change the orientation of a molecule. A stable molecule may not need to much energy to be distorted. From Table 2. it is seen that HDDH has the least deformation energy at geometry optimization showing how stable it is at that state. Our comparison is based on the equilibrium state, and it can be seen that HDDH has the least energy of deformation at 60 °C. This confirms the stability of the HDDH molecule stated earlier concerning the energy of the molecule. The van der Waal accessible surface or solvent accessible surface area is the surface area of a biomolecule that is accessible to a solvent. Table 2. shows the van der Waal accessible surface for HDDH, and it is seen that HDDH has a larger surface area at 60 °C, this may contribute to the adsorption/corrosion inhibitive potential of HDDH at that temperature. The electronegativity values of HDDH at the two temperatures is less than the electronegativity of iron which is 7.0 eV, this signifies that

electrons will flow freely from the HDDH to the iron surface. Global hardness and softness are basic chemical concept called Global reactivity and has been theoretical justified within the framework of DFT [26]. Chemical hardness signifies the resistance towards the deformation of the electron cloud of the atoms. Soft molecules are more reactive than hard molecules because they can easily give electrons to an acceptor. A hard molecule has a large energy gap and a soft molecule has a small energy gap [27]. Table 2. shows clearly from the calculation that HDDH have the lowest hardness and highest softness values at 60 °C compared to the values at 80 °C. The number of electron transfer (ΔN) was also calculated as seen in Table 2. These values of ΔN shows that the adsorption/corrosion inhibitive potential resulting from electron donation agrees with Lukovits's study [28] which is if $\Delta N < 3.6$, the adsorption/corrosion inhibitive potential increases by increase electron donating ability of the molecule to donate electrons to the iron surface. Higher fraction of electron transfer indicates better adsorption/corrosion inhibitive potential and this was archived at 60 °C. The electrophilic power of HDDH is higher at 80 °C, that is the higher the ability of HDDH to accept electron from the iron surface which can aid adsorption. But due to the fact that the fraction of electron transfer ($\Delta N < 3.6$) the adsorption is mainly caused by the donation of electrons by HDDH to the iron surface. So, a higher electrophilic power is not too relevant in this context.

3.2.1 Local Selectivity

To ascertain the active sites of a molecule, three factors have to be considered and they are the natural atomic charge, the distribution of the frontier molecular orbital and the Fukui indices [10]. Local reactivity is analyzed by means of the condensed Fukui function. This allows us to differentiate each part of the molecule based on their distinguished chemical behavior due to the different substituent functional groups present. The electrophilic and nucleophilic attack is controlled by the highest values of f_k^- and f_k^+ . The calculated Fukui indices values for electrophilic and nucleophilic attack for HDDH is shown in Table 3. (only the more concerned atoms C, N and O are quoted) and the sites for electrophilic and nucleophilic attack is shown plotted on the molecules in Fig. 6.

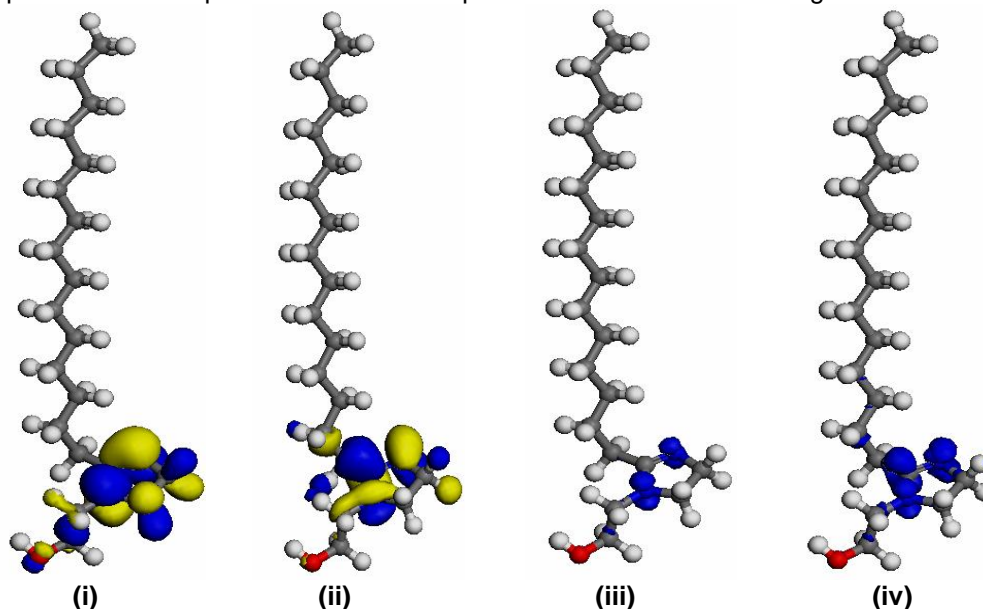


Fig. 6. (i) HOMO orbital plot (ii) LUMO orbital plot (iii) Plot for Fukui Negative sites for electrophilic attack (iv) Plot for Fukui Positive sites for Nucleophilic attack for HDDH.

322 **Table 3. Fukui negative (f_k^-) and positive (f_k^+) indices values for HDDH at Geometry**
 323 **optimization, 60 °C and 80 °C**
 324

Atom	Fukui Negative (f_k^-) values			Fukui Positive (f_k^+) values		
	Geo Opt	60 °C	80 °C	Geo Opt	60 °C	80 °C
O1	0.046	0.020	0.032	0.023	0.016	0.026
C2	-0.011	-0.010	-0.012	-0.015	-0.007	-0.010
C3	-0.041	-0.051	-0.052	-0.045	-0.041	-0.038
N4	0.142	0.160	0.129	0.009	0.018	0.006
C5	-0.041	-0.040	-0.038	-0.025	-0.027	-0.028
C6	-0.036	-0.028	-0.031	-0.036	-0.032	-0.035
N7	0.172	0.165	0.185	0.136	0.142	0.137
C8	0.027	0.024	0.033	0.139	0.154	0.157
C9	-0.017	-0.018	-0.010	-0.042	-0.041	-0.022
C10	-0.013	0.000	-0.018	-0.053	-0.037	-0.036
C11	-0.009	-0.002	-0.006	-0.014	-0.008	-0.017
C12	-0.005	-0.005	-0.008	-0.010	-0.008	-0.011
C13	-0.005	-0.005	-0.011	-0.006	-0.007	-0.011
C14	-0.004	0.001	0.000	-0.005	0.000	-0.001
C15	-0.003	-0.007	-0.007	-0.003	-0.008	-0.007
C16	-0.002	-0.002	-0.002	-0.003	-0.002	-0.002
C17	-0.001	-0.002	-0.001	-0.002	-0.002	-0.001
C18	-0.002	-0.002	-0.002	-0.002	-0.002	-0.002
C19	-0.001	-0.001	-0.003	-0.001	-0.001	-0.003
C20	-0.001	0.001	-0.002	-0.001	0.001	-0.002
C21	-0.001	0.000	-0.002	-0.001	0.000	-0.002
C22	-0.001	0.000	-0.002	-0.001	0.000	-0.002
C23	-0.001	-0.001	0.000	-0.001	-0.002	0.000

325
 326 From Table 3. it is observed that higher values of f_k^- is possessed by the N4 and N7 atoms
 327 at geometry optimization and at 60 °C and 80 °C, with the N7 having the highest value it is
 328 said to be the major atom for electrophilic attack. Higher values for f_k^+ is possessed by the
 329 N7 and C8 atoms at geometry optimization and at 60 °C and 80 °C, with the C8 having the
 330 highest value it is said to be the major atom for nucleophilic attack.

331 332 333 **4. CONCLUSION**

334
 335 From the molecular dynamic simulation, HDDH is attached to the iron surface using
 336 the ring part of the molecule. HDDH shows different conformation in its structure at the two
 337 temperatures studied which is due to changes in the bond length of the atoms present, other
 338 factors not reviewed includes bond angle and torsional strain. From the quantum chemistry
 339 calculations and considering the natural atomic charge, the frontier molecular orbital plots,
 340 the Fukui indices values and plots and the bond length analysis, the Main active site for
 341 adsorption of HDDH is the N=C-N region in the ring. Considering both the molecular
 342 dynamic simulation and the quantum chemistry calculation HDDH is found to adsorb/inhibit
 343 better at 60 °C. This study supports the statement made in the introductory part of this
 344 research paper about the inhibition efficiency of a molecule that is physically adsorb on a
 345 metal surface.

346
 347

348 **COMPETING INTERESTS**

349

350 Authors have declared that no competing interests exist.

351

352

353

354 **REFERENCES**

355

356 1 Bastidas JM, Damborenea J, Vazquez AJ. Butyl substituents in n-butylamine and their
357 influence in mild steel corrosion inhibition in hydrochloric acid. Journal of Applied
358 Electrochemistry. 1997; 27:345-349.

359 2 Maghraby AA, Soror TY. Quaternary ammonium salt as effective corrosion inhibitor for
360 carbon steel dissolution in sulphuric acid media. Advanced in Applied Science Research.
361 2010. 1;143.

362 3 Shhiri A, Etman M, Dabosi F. Electro and physicochemical study of corrosion inhibition of
363 carbon steel in 3% NaCl by alkylimidazoles. Electrochimica Acta. 1996. 41; 429.

364 4 Abd El-Rehim SS, Ibrahim MA, Khaled FF. 4-Aminoantipyrine as an inhibitor of mild steel
365 corrosion in HCl solution. Journal of Applied Electrochemistry. 1999; 593-599,

366 5 Okafor PC, Ebiekpe VE, Azika CF, Egbung GE, Brisibe EA, Ebenso EE. Inhibitory action
367 of *Artemisia annua* extracts and *artemisinin* on the corrosion of mild steel in H₂SO₄
368 solution. International Journal of Corrosion.doi:10.1155/2012/768729

369 6 Kabanda MM, Murulana LC, Ozcan M, Karadag F, Dehri I, Obot IB, Ebenso EE. Quantum
370 chemical studies on the corrosion inhibition of mild steel by some Triazoles and
371 Benzimidazole Derivatives in acidic medium. International Journal of Electrochemical
372 Science. 2012; 5035-5056.

373 7 Udhayakala P, Rajendiran S, Gunasekaran S. Quantum chemical studies on the
374 efficiencies of vinyl imidazole derivatives as corrosion inhibitors for mild steel. Journal of
375 Advanced Scientific Research. 2012; 37-44.

376 8 Zarrouk A, El-Quali I, Bouachrine M, Hammouti B, Ramli Y, Essassi E, Warad I, Aounti A,
377 Salghi R. Theoretical approach to the corrosion inhibition efficiency of some Quinoxaline
378 derivatives of steel in acid media using the DFT method. Research on Chemical
379 Intermediates. 2013;1125-1133.

380 9 Zhu J, Chen S. A theoretical investigation on the inhibition efficiencies of some Schiff
381 bases as corrosion inhibitors of steel in Hydrochloric acid. International Journal of
382 Electrochemical Science. 2012; 11884-11894.

383 10 Xia S, Qui M, Yu L, Lui F, Zhao H. Molecular dynamics and density function theory study
384 on relationship between structure of imidazoline derivatives and inhibition performance.
385 Corrosion Sciences. 2008; 2012-2029.

386 11 Musa YA, Ramzi TT, Mohamed AB. Molecular dynamic and quantum chemical
387 calculations for phthalazine derivatives as corrosion inhibitors of mild steel in 1M HCl.
388 Corrosion Science. 2012; 176-183.

389 12 Delley B. Modern density functional theory. Elsevier Science, Amsterdam; 2000.

390 13 Liu J, Yu W, Zhang J, Hu S, You L, Qiao G. Molecular modelling study on inhibition
391 Performance of imidazolines for mild steel in CO₂ corrosion. Applied Surface Science.
392 2010. 256; 4729-4733.

393 14 Koopmans T. Koopmans theorem in statistical Hartree-fock theory. Physica. 1933; 104-
394 113.

395 15 Parr RG, Pearson RG. Absolute hardness: companion parameter to absolute
396 electronegativity. Journal of the America Chemical Society. 1983; 7512-7516.

397 16 Pearson RG. Inorganic Chemistry. Elsevier, Amsterdam; 1988.

398 17 Parr RG, Szentpaly L, Liu S. Electrophilicity index. Journal of the America Chemical
399 Society. 1999; 121:1922.

400 18 Yang W, Mortier W. The use of global and local molecular parameters for the analysis of

- 401 the gas phase basicity of amines. Journal of the America Chemical Society. 1986; 5708-
402 5713.
- 403 19 Quijano MA, Pardav MP, Cuan A, Romo, MR, Silva GN, Bustamante RA, Lopez AR,
404 Hernandez HH. Quantum Chemical study of 2-Mercaptoimidazole, 2-
405 Mercaptobenzimidazole, 2-Mercapto-5-Methylbenzimidazole and 2-MeRcapto-5-
406 Nitrobenzimidazole as corrosion inhibitors for steel. International Journal of
407 Electrochemical Science. 2011; 6: 3729-3742.
- 408 20 Roger N. An introduction to surface chemistry. Queen Mary. London; 2006.
- 409 21 Hellsing B. Surface physics and Nano science physics. Goteborg University, Sweden;
410 2008.
- 411 22 Yurt A, Ulutasa S, Dal H. Electrochemical and theoretical investigation on the corrosion of
412 aluminium in acidic solution containing some Schiff bases. Applied Surface Science.
413 2006; 253:919-925.
- 414 23 Eddy NO. Theoretical study on some amino acids and their potential activity as corrosion
415 inhibitors for mild steel. Molecular Simulation. 2010; 36:5.
- 416 24 Obot IB, Obi-Egbedi NO, Ebenso EE, Afolabi AS, Oguzie EE. Experimental, quantum
417 chemical calculations and molecular dynamic simulation insight into the corrosion
418 inhibition properties of 2-(6-methylpyridin-2-yl) oxazole [5,4-f][1,10]phenathroline on mild
419 steel. Research on Chemical Intermdiates. 2012; 1927-1948.
- 420 25 Ekpo VF, Okafor PC, Ekpe UJ, Ebenso EE. Molecular dynamics simulation and quantum
421 chemical calculations for the adsorption of some thiosemicarbazone (TSC) derivatives on
422 mild steel. International Journal of Electrochemical Science. 2011; 1045-1057.
- 423 26 Udhayakala P. Quantum chemical studies on the inhibition potentials of thiophene
424 derivatives for the corrosion inhibitors of carbon steel. Journal of Chemical and
425 Pharmaceutical Research. 2015; 7(1):803-810.
- 426 27 Obi-Egbedi NO, Obot IB, El-Khaiary MI, Umoren SA, Ebenso EE. Computational
427 simulation and statistical analysis on the relationship between corrosion inhibition
428 efficiency and molecular structure of some phenathroline derivatives on mild steel
429 surface. International Journal of Electrochemical Science. 2011; 5649-5675.
- 430 28 Lukovits I, Kalman E, Zucchi F. Corrosion inhibitors-correlation between electronic
431 structure and efficiency. Corrosion. 2001; 3-8.